

Delay Analysis and Buffer Optimization for Priority-Aware Networks-on-Chip (NoC)

Baoliang Li, Zeljko Zilic, Wenhua Dou,

Abstract—Among all the implementation alternatives of Networks-on-Chip (NoC), priority-aware wormhole-switched NoC is promising to meet both the worst-case and average-case latency requirements of on-chip communication. The worst-case end-to-end latency and buffer requirement analysis are very important for the development of real-time applications on this platform. In this paper, we first build a Real-Time Calculus (RTC) based performance model for the priority-aware wormhole-switched NoC. Then, we propose an end-to-end latency analysis algorithm and a buffer optimization algorithm based this model. The latency analysis algorithm can give much tighter delay bound than the existing deterministic network calculus method, since it take the maximum service capacity and minimum arrival traffic into consideration. The buffer optimization algorithm try to reduce the buffer space required for each flow without violating the deadline, which improves the existing backlog bound obtained by link-level buffer-space analysis method. Our algorithms are topology-independent, they take as input the network topology graph and the application traffic characterization, and give the end-to-end latency bound and buffer requirement for each traffic flow. Our model enables the fast performance evaluation and buffer optimization of priority-aware wormhole-switched NoC, which can be used for application mapping, routing selection and power reduction. Experiment results demonstrate the effectiveness and tightness of our model. In addition, further comparisons with other theoretical models also indicates that, our method outperforms the existing methods while the tightness of the derived delay and backlog bound are considered.

Keywords—Networks-on-Chip (NoC), priority-aware, real-time calculus, delay bound, buffer optimization

I. INTRODUCTION

The conventional on-chip interconnection paradigms, e.g. bus, ring and point-to-point links, are not able to meet the strict and complex communication requirements of modern large scale Chip-MultiProcessors (CMPs) and System-on-Chip (SoC). As an alternative, Networks-on-Chip (NoC) is proposed to provide better scalability and higher power efficiency. As a key component of CMPs and SoC, NoC must be well designed to meet the rigorous requirements on performance and design cost. Although various proposals have been emerged, each focusing on improving different performance metrics of on-chip interconnects, e.g. end-to-end latency, throughput and power, most of the existing research on NoC are focusing on the improvement of average performance, and simulation is the most widely used performance evaluation method. Whereas,

Baoliang Li and Wenhua Dou are with the College of Computer Science, National University of Defense Technology, Changsha 410073, P.R. China
 Zeljko Zilic are with Department of Electrical & Computer Engineering, McGill University, Montreal H3A-2A7, Quebec, Canada

Manuscript received XX XX, 2014; revised XX XX, 2014.

there also exists lots of on-chip applications, which are sensitive to the worst-case or real-time communication performance of NoC, e.g. cache coherent protocol [1] and multimedia application [2]. How to design the on-chip communication infrastructure for these applications and analyze its feasibility are of a big challenge for the researchers.

To meet the rigorous Quality-of-Service (QoS) requirement, various special hardware implementations have been proposed, e.g. Time-Division Multiplexing-Access (TDMA) [3], circuit-switch [4] and time-triggered switch [5]. Although provide strict real-time communication guarantee, the average performance and resource utilization of these proposals are very poor. In contrast, wormhole-switched NoC is widely used in on-chip network due to its simplicity and high-efficiency. Thus, providing real-time communication support on the conventional wormhole-switched NoC to meet both average-case and worst-case communication requirements is the most promising solution. To achieve this goal, a special scheduling policy (e.g. DifServ [6] or priority-aware implementation [7][8][9]) or flow control mechanism (e.g. [10][11]) should be integrated into the conventional wormhole-switched NoC. For all these wormhole-switch based real-time communication proposals, a key step before their adoption as the platform of real-time applications is the analysis of the worst-case communication latency for all the real-time flows to guarantee the satisfaction of deadline constraint. An effective buffer analysis approach is also needed to optimize the buffer allocation under real-time constraint, since buffer usually consumes about 46% power [12] and occupies 30% area [13] of entire router.

A creditable and accurate worst-case analysis is crucial for the application of wormhole-switched NoC in real-time communication, since an over optimistic estimation will lead to the violation of deadline, while an over pessimistic estimation will make the utilization of on-chip resource very low. The conventional simulation method is not competent for the worst-case performance analysis, because the worst-case scenarios are hard to be captured by simulation. As an alternative, the analytical method can establish the relationship between performance metrics and design parameters in a very short time, and give the worst-case performance immediately. For the worst-case analysis of fixed-priority wormhole-switched on-chip networks, Flow-Level Analysis (FLA) [7], Link-Level Analysis (LLA) [14][15] and Deterministic Network Calculus (DNC) [16] have been successfully applied. Both FLA and LLA have their roots in the classic scheduling theory, which assume that, the traffic flows are strictly periodic, and the input buffer of wormhole-switched NoC is sufficient large, so that

the back-pressure caused by flow control can be ignored. In addition, they simplify the router model by restricting the per-hop latency to be one cycle, which is complying with the conventional router implementation.

Deterministic network calculus based method [16] can overcome all these limitations by applying the advanced operators in dioid algebra. However, we found that the DNC based performance bound in [16] can be further improved if we take the maximal service curve of on-chip routers and minimal arrival curve into consideration. These two curves can be used to improve the tightness of output arrival curve and leads to a tighter leftover service curve at the downstream routers. The improved leftover service curve further tighten the obtained performance bounds for low-priority flows. Motivated by this observation, we adopt the real-time calculus (RTC) theory [17] originally used for the real-time analysis of task scheduling to build an end-to-end performance model for the wormhole-switched NoC with credit-based flow control. Compared with the DNC model in [16], our model can significantly improves the tightness of performance bounds, we will further explain the reason and demonstrate the improvement in Section V. The main contribution of this paper is two folded: (1) We propose an end-to-end latency analysis algorithm for the priority-aware wormhole-switched NoC based on the RTC model. The output of this algorithm can be used as the reference of IP core mapping, task mapping, routing selection, or NoC parameters configuration; (2) We also propose an RTC based buffer optimization algorithm for the priority-aware wormhole-switched NoC to reduce the buffer size under deadline constraint. This is a significant improvement of previously proposed FLA and LLA based buffer optimization method [15], which can be used to minimize the power consumption and chip area.

The rest of this paper is organized as follows: we present the existing real-time communication proposals and its related performance analysis methods in Section II. In Section III, the basic assumptions on priority-aware wormhole-switched NoC and a brief introduction to RTC theory is presented. The detailed modeling process is presented in Section IV, where we also propose the end-to-end latency analysis algorithm and buffer optimization algorithm. We present the experiment results and comparison with other analytical methods in Section V. Finally, we summarize our paper in Section VI.

II. RELATED WORK

Since first introduced in 2001 [18], various NoC proposals have been emerged to meet different on-chip communication requirements. The main requirements posed to NoC by on-chip applications are latency and bandwidth. To meet these demand, NoC are designed to be either best-effort or guaranteed-service, depending on the hardware cost and application requirements. Best-effort NoC can make better use of the on-chip shared resource, but it does not necessarily provide any performance guarantee for the applications. To provide guaranteed-service for different applications, a simple and effective solution is classifying these applications into several service classes, each with different priorities, and the network provides services according to the priority of each class. Representative implementations of this idea include QNoC [25],

fixed-priority NoC [7] and AEthereal [3] etc. The performance evaluation method for both best-effort and guaranteed service NoC include the average analysis and worst-case analysis. For the average analysis, simulation- and probability-based method hold the dominant position for both of these two categories. However, for the worst-case analysis, simulation is not competent due to the difficulty in covering all the corner cases. The analytical worst case analysis for these two categories is also slightly different.

Synchronous Data Flow (SDF) graph [19] and DNC [20] have been presented to model the worst case performance bound of best-effort NoC. The former method assumes the traffic flow to be periodical, and the latter one eliminates this constraint to allow the traffic to be arbitrary patterns. In [20], the authors build an analytical performance model with DNC taking the various contention and flow control into consideration. This result is further extended in [21], where the traffic splitter is proposed to support the multi-path routing polices. Another method is presented in [22] to compute the worst-case latency for conventional wormhole switched network, and a real-time Wormhole Channel Feasibility Checking (WCFC) algorithm is proposed. This research is further extended to calculate the bandwidth and latency bounds in [23], and used for topology synthesis of best-effort NoC in [24].

In [26], contention tree model was proposed to analyze the feasibility of real-time traffic delivered by priority-aware wormhole-switched NoC. It improves the previous results, e.g. lumped link model [11] and dependency graph model [8], by allowing the concurrent link usage. This is similar as the the LLA [14], which improves the FLA proposed in [7] by treating each link segment separately. A comprehensive comparison among FLA, contention tree model [26], lumped link model [11] and dependency graph model [8] can be found in [27], in which several defects of previous works [26][11][8] are illustrated and the advantages of FLA are highlighted. Two buffer sizing method based on FLA and LLA, i.e. Flow-Level Buffer-space Analysis (FLBA) and Link-Level Buffer-space Analysis (LLBA), are proposed in [15] to estimate the buffer size of priority-aware wormhole-switched NoC. The main drawback of FLA and LLA is that, both these two methods require the traffic arrive periodically and assume the router has single cycle latency, which are of significant simplification to the realistic traffic pattern and router implementation. In addition, the FLBA and LLBA can only compute the minimum backlog bound at each router which does not trigger the flow control. In fact, we can further reduce the buffer size as long as the the flow control does not cause the violation of deadline.

On the other hand, although the DNC based analytical method for best-effort NoC proposed in [20] can be applied to the analysis of priority-aware wormhole-switched NoC, the obtained performance bounds is very conservative, especially for the high priority flows. This is because, it does not take the priority-aware scheduling into consideration. To overcome this limitation, an DNC model is proposed to analyze the worst case latency of priority-aware wormhole-switched NoC in [16]. But we found that, the DNC method in [16] can be further improved if we take the maximum service curve of each router and minimum arrival curve of each flow into con-

sideration, because the maximal service curve and minimum arrival curve can limit the output arrival curve and improve the leftover service curve for low-priority flows (please refer to Theorem 1.6.2 in [28] for the reason). Motivated by this observation, we adopt the RTC theory [17] to build the worst-case performance model for the priority-aware wormhole-switched NoC. Real-time calculus is the extension of DNC theory by integrating the maximum service curve and minimal arrival curve, which has been widely used in the modeling and analysis of network processor [29], CAN [30], FlexRay [31] and DSP systems [32], etc. To ease the application of RTC, a real-time calculus toolbox [33] has also been implemented to support the numerical calculation.

III. PRELIMINARIES

A. Basic Assumptions

In this paper, we consider the same network model as the priority-aware wormhole-switched NoC proposed in [9][7][11][14]. Each router has the same number of input and output port, and each input port has sufficient FIFO buffers, i.e. Virtual Channel (VC), to accommodate all the incoming traffic of different priority level. The allocation of VC is determined by the VC allocator. To ensure the predictable transmission of message, we assume that, a deterministic routine computation module is used to determine the output port of each communication message. Crossbar is used to switch traffic from input ports to the output ports, and the switch operation is determined by the switch allocator. The switch allocator is priority-aware: if multiple flits from different input ports or different VCs of the same input port contend for the same output port, it will only grant the flit with highest priority. Flits from a lower priority can transmit a flit if and only if there are no flits from higher priority in the input buffer or the flits with higher priority are self-blocked due to the insufficiency of VC buffer at downstream router. In addition, we also assume that, the buffer depth of each VC is finite, and credit-based flow control is adopted between each router.

The router micro-architecture considered in this paper has 5 pipeline stages, i.e. Buffer-Write (BW), Route Computation (RC), VC Allocation (VA), Switch Allocation (SA), Switch Traversal (ST) and Link Traversal (LT). For the detailed description of the implementation and functionality of the router micro-architecture, please refer to [34]. Although we focus on the standard 5-stage router, our method can be easily modified to support the speculation-based router, e.g. routers with only 2 or 3 stages, the only difference is the initial delay of our model. We will demonstrate the adoption of our model in a single cycle router in Section V. Communication message is broken input packets, and each packet is composed of one head flit, one tail flit and several body flits. Each head flit should traverse all the five stages to find a path and reserve VC for the follow non-head flits. Non-head flits skip the RC and VA stage since the routine and VC have been determined by head flit. Router resource and control information reserved for a packet will be released only after the tail flit of this packet has been departed from the router. An additional priority field in the head flit is required for the routers to scheduling multiple

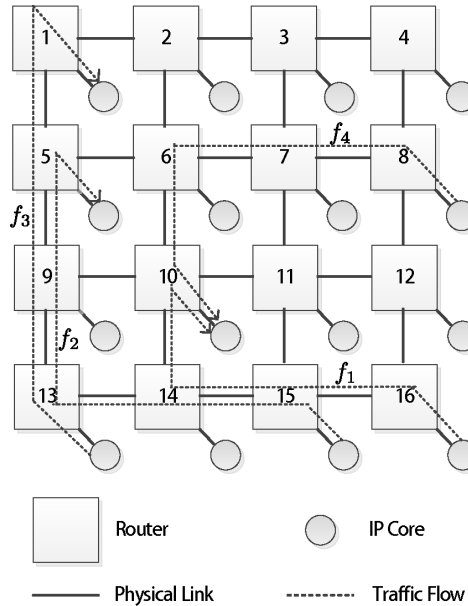


Fig. 1: Mesh topology with 4 real-time traffic flows

contending flows according to their priority. To simplify of our analysis, we also assume that, the entire chip use synchronous design, the frequency and period of clock are f and T , respectively. Our method can also be applied to analyze Global Asynchronous Local Synchronous (GALS) NoC with little modification, because the routers located in different voltage-frequency islands can be synchronized with a half cycle synchronizer [35], corresponding to a fixed-latency element in DNC theory.

Our performance model is topology independent, but to demonstrate the basic idea of our method, we take the mesh topology shown in Fig. 1 as examples throughout this paper. The router in mesh topology has five ports, corresponding to the four cardinal directions (West, East, North and South) and the Network Interface (NI), which connects to the local Intellectual Property (IP) core. There are 4 traffic flows in Fig. 1, i.e. f_1 , f_2 , f_3 and f_4 . A flow is a sequence of packets with the same transmission path, source address and destination address. The path of a traffic flow is defined as a router chain started from source NI and ended at destination NI. We must emphasize that, although there is only four flows in the network, it is sufficient to demonstrate our the idea of our method, and our method can handle more traffic flows efficiently. To ensure the low latency transmission for real-time traffic flows, we have to assign higher priorities to these flows. As the minimum transmission unit in NoC is flit and a higher priority packet can preempt the transmission of a lower priority packet, the NoC architecture considered in this paper is flit-level preemptive [22]. Our method extends the existing methods in [14][16] to allowing multiple flows share the same priority. Flits from different flows with the same priority are served in round-robin order.

B. Introduction to Real-Time Calculus

Real-time calculus is an extension of DNC [17], by adding the upper service curve and lower arrival curve to describe the maximal service capacity of processing elements and minimal arrival rate of events. It is the mathematical basis of Modular Performance Analysis (MPA) [36] technique used for real-time task scheduling. Here we only present the definition of RTC arrival curve and service curve, for more details about this theory, please refer to [17].

Definition 1 (Real-Time Arrival Curve [17]): Let $R[s, t]$ denote the number of events that arrived within the time interval $[s, t)$. The lower bound and upper bound on $R[s, t)$ is called the lower arrival curve α^l and upper arrival curve α^u , which satisfy

$$\alpha^l(t-s) \leq R[s, t) \leq \alpha^u(t-s), \forall s < t$$

where $\alpha^l(0) = \alpha^u(0) = 0$. The RTC arrival curve for R is denoted as $\langle \alpha^l, \alpha^u \rangle$ for short.

From the definition, we find that the upper arrival curve (corresponding to the arrival curve of DNC [28]) and lower arrival curve are used to characterize the upper and lower bound of arrived events within any time interval Δ .

Definition 2 (Real-Time Service Curve [17]): Let $S[s, t)$ denote the total number of events that can be processed by the system in the time interval $[s, t)$. The lower bound and upper bound on $S[s, t)$ is called the lower service curve β^l and upper service curve β^u , which satisfy

$$\beta^l(t-s) \leq S[s, t) \leq \beta^u(t-s), \forall s < t$$

where $\beta^l(0) = \beta^u(0) = 0$. The RTC service curve for S is denoted as $\langle \beta^l, \beta^u \rangle$ for short.

From the definition of RTC service curve, we find that the upper and lower service curve are corresponding to the maximal service curve and service curve in DNC theory [28], respectively. Thus, the concatenation theorems for service curve (see Theorem 1.46 in [28]) and maximal service curve (see Theorem 1.6.1 in [28]) are also applicable to the RTC service curve. In this paper, we will utilize the discrete time RTC arrival curve and service curve to characterize the arrived traffic and service capacity, since the minimal time unit in the wormhole-switched NoC is clock period T . Events in arrival curve and service curve refer to the arrival and service of flits, respectively. If we obtain the arrival curve $\langle \alpha^l, \alpha^u \rangle$ of a specific traffic flow and the service curve $\langle \beta^l, \beta^u \rangle$ provided to this flow, we can get the output arrival curve $\langle \alpha'^l, \alpha'^u \rangle$ of this flow and leftover service curve $\langle \beta'^l, \beta'^u \rangle$ for the other flows with the following equations [17]:

$$\alpha'^l = \min\{(\alpha^l \oslash \beta^u) \otimes \beta^l, \beta^l\} \quad (1)$$

$$\alpha'^u = \min\{(\alpha^u \otimes \beta^u) \oslash \beta^l, \beta^u\} \quad (2)$$

$$\beta'^l = (\beta^l - \alpha^u) \bar{\otimes} 0 \quad (3)$$

$$\beta'^u = \max\{(\beta^u - \alpha^l) \bar{\otimes} 0, 0\} \quad (4)$$

where $\otimes, \oslash, \bar{\otimes}, \bar{\oslash}$ are corresponding to the min-plus convolution, de-convolution, and max-plus convolution and de-convolution [28], respectively.

After we obtained the arrival curve $\langle \alpha_{f_i}^l, \alpha_{f_i}^u \rangle$ of traffic flow f_i and the service curve $\langle \beta_{R_j, f_i}^l, \beta_{R_j, f_i}^u \rangle$ provided by each router R_j to flow f_i on its path, we can obtain the end-to-end latency and backlog bound by the following equations,

$$\text{Delay}(f_i) = H(\alpha_{f_i}^u, \beta_{R_1, f_i}^l \otimes \beta_{R_2, f_i}^l \otimes \cdots \otimes \beta_{R_N, f_i}^l), \quad (5)$$

$$\text{Backlog}(f_i) = V(\alpha_{f_i}^u, \beta_{R_1, f_i}^l \otimes \beta_{R_2, f_i}^l \otimes \cdots \otimes \beta_{R_N, f_i}^l) \quad (6)$$

where operators $H(\cdot, \cdot)$ and $V(\cdot, \cdot)$ mean the maximal vertical and horizontal deviation, respectively.

IV. DELAY ANALYSIS AND BUFFER OPTIMIZATION

In this section, we first build the RTC model for the priority-aware wormhole-switched NoC, then, we propose an end-to-end latency analysis algorithm and a buffer optimization algorithm based on the constructed RTC model. This model consists of two parts, i.e. traffic model and service model. We will introduce two method to obtain the traffic model in subsection IV-A. The service model is slightly complicated than the traffic model. While constructing the service model for priority-aware wormhole-switched NoC, the follow four aspects should be considered: (1) Only the head flit need to be processed by RC and VA stage, the subsequent flits of a packet just follow the data-path built by head flit. To simplify our RTC model, we need specific mechanism to characterize the service provided to head and non-head flits in a unified way. (2) Our model extends the existing approach [14][16] by allowing priority sharing between flows. Thus, the leftover service curve provided to lower-priority flows can only be derived after the service curves of all the high-priority flows have been calculated. (3) Due to the limited on-chip buffer, credit-based flow control is used as a back-pressure mechanism to prevent buffer overflow. Before analysis the end-to-end performance with Eq.(5) and Eq.(6), we should first break the cyclic-dependence caused by flow control. (4) To guarantee the tightness of our theoretical performance bounds and simplify the numerical computation, we should apply the concatenation theorems as far as possible. But, this concatenation process becomes complicated when the credit-based flow control is taken into consideration. We will discuss the first two issues in subsection IV-B, and the last two issues are discussed in subsection IV-C and subsection IV-D, respectively. The latency analysis algorithm and buffer optimization algorithm are introduced in subsection IV-E and subsection IV-F, respectively.

A. Traffic Model

In a NoC connected CMP or SoC system, the communication between each pair of IP cores was realized by transmitting packets, and the packet is further divided into flits, which is the minimum transmission unit in wormhole-switched NoC. Denote $\langle \alpha^l(\Delta), \alpha^u(\Delta) \rangle$ the arrival curve of a flow, we can extract the arrival curve from the synthetic traffic or communication trace with the sliding window method [17]. For each window size Δ , this method tries to find the maximal and minimal number of arrived flits (corresponding to $\alpha^l(\Delta)$ and $\alpha^u(\Delta)$) by analyzing the time series of flits. The arrival

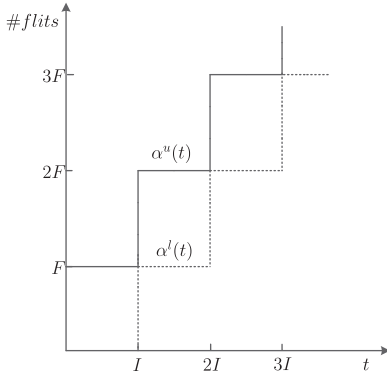


Fig. 2: Real-time calculus arrival curve for periodically arrived traffic with period I and packet length F . The solid line and dotted line represent the upper arrival curve and lower arrival curve, respectively.

curve obtained by this method might not be periodic, but it does not hamper the application of RTC theory. As has been presented in subsection III-B, the service model considered in this paper is a flit-by-flit system. To compute the worst-case end-to-end packet latency for a flow, the obtained arrival curve must be L -packetized [28]. Denote L_{max} the maximum packet length (in flits) of a flow, $R(t)$ the accumulative arrival function, and $\mathcal{P}^L(\cdot)$ the L -packetizer operator, we have [28]

$$R(t) - l_{max} \leq \mathcal{P}^L(R(t)) < R(t)$$

and

$$R(s) - l_{max} \leq \mathcal{P}^L(R(s)) < R(s)$$

which indicate

$$\alpha(t-s)^l - l_{max} < \mathcal{P}^L(R(t)) - \mathcal{P}^L(R(s)) < \alpha(t-s)^u + l_{max}.$$

The inequalities above indicate that, if a flow has an arrival curve $\langle \alpha^l(\Delta), \alpha^u(\Delta) \rangle$, the L -packetized flow has a arrival curve $\langle \alpha^l(\Delta) - l_{max}1_{\{\Delta>0\}}, \alpha^u(\Delta) + l_{max}1_{\{\Delta>0\}} \rangle^1$. We can also directly obtain the L -packetized arrival curve instead of transformation from flit arrival curve for some special cases. For example, suppose all the packets have the same length F and arrived periodically with period I . Then, the flit arrival curve of this flow can be obtained by simply amplifying the arrival curve for periodic event stream provided in [17] at y -axis with a factor F , as shown in Fig. 2. The alert readers would notice that, the flit arrival curve obtained by this way is also L -packetized arrival curve $\mathcal{P}^L(\alpha)$, which can be used to compute the end-to-end packet latency directly.

B. Router Model

While modeling the service capacity of routers with RTC, we can analyze the data-path of a flow stage-by-stage. After obtained the service curve for each stage, the service curve provided by the router to the flow can be obtained by concatenating all the service curves of these five stages. This is significantly different with the existing DNC based model

[20], [16], where they treat the entire router as a whole and designate a Latency-Rate (LR) service curve for simplicity. The advantage of our method is that, it can be easily modified to characterize the non-standard router micro-architectures, by simply letting the service curve of non-existed stages to be burst delay function $\delta_0(t)^2$. Next, we try to obtain the service curves of all these 5 stages:

(1) BW stage and ST stage: all the flits within a traffic flow will traverse these two stages, and experience a fixed delay T . Take the BW stage as an example, for any time interval of length less than T , the maximum and minimal number of flits that can be seen are one and zero, respectively, since it outputs one flit at each cycle T . Similarly, for any time interval of length greater than T , the maximum and minimal number of flits that can be seen are two and one, respectively. The resulted service curves, i.e. $\langle \beta_{BW}^l, \beta_{BW}^u \rangle$ and $\langle \beta_{ST}^l, \beta_{ST}^u \rangle$, are shown in Fig. 3a.

(2) RC stage and VA stage: the traverse latency of head flit and non-head flits at these two stages are T and 0, respectively. A sophisticated solution to construct a unified service curve for head flit and non-head flits at these two stages is that, we can view these two stages can service an entire packet within T period. Suppose the packet length is F , the equivalent service curve for these two stages, i.e. $\langle \beta_{RC}^l, \beta_{RC}^u \rangle$ and $\langle \beta_{VA}^l, \beta_{VA}^u \rangle$, can be easily obtained by amplifying the service curve of Fig. 3a in y -axis with a factor F , as shown in Fig. 3b.

(3) SA stage: each output port in the wormhole-switched NoC has a SA scheduler to schedule the switch traversal at each cycle. Thus, following the same approach as BW and ST stage, we can get the service curve $\langle \beta_{SA,R_i,f_j}^l, \beta_{SA,R_i,f_j}^u \rangle$ provided by SA stage of router R_i to all the contention flows, as shown in Fig. 4a. For the fixed-priority based scheduling policy, switch allocators provide service for high priority flows first, and flows with the same priority will be served with Round-Robin order. The unserved flows will be imposed an additional latency T due to the failure of switch arbitration.

Denote by $\langle \beta_{SA,R_i,f_j}^l, \beta_{SA,R_i,f_j}^u \rangle$ the service curve provided to flow f_j by SA stage of router R_i , the equivalent service curve of router R_i provided to f_j , i.e. $\langle \beta_{R_i,f_j}^l, \beta_{R_i,f_j}^u \rangle$, can be obtained by concatenating the service curves of all the 5 stages together:

$$\begin{aligned} \beta_{R_i,f_j}^l &= \beta_{BW}^l \otimes \beta_{RC}^l \otimes \beta_{VA}^l \otimes \beta_{SA,R_i,f_j}^l \otimes \beta_{ST}^l, \\ \beta_{R_i,f_j}^u &= \beta_{BW}^u \otimes \beta_{RC}^u \otimes \beta_{VA}^u \otimes \beta_{SA,R_i,f_j}^u \otimes \beta_{ST}^u. \end{aligned}$$

The alert readers would notice that, the contention of different flows only occurs at SA stage. Thus, if we obtained the service curve provided by SA stage to flow f_j , we can obtain the service curve of router directly. Suppose the total service curve provided by SA stage is $\langle \beta_{SA,R_i}^l, \beta_{SA,R_i}^u \rangle$ and the leftover service curve after serving flows with higher priority than f_j is $\langle \beta_{SA,R_i}^{l'}, \beta_{SA,R_i}^{u'} \rangle$, to obtain the service curve $\langle \beta_{SA,R_i,f_j}^l, \beta_{SA,R_i,f_j}^u \rangle$, we should consider the following two cases:

(a) all the flows contending with f_j at R_i have lower priorities. For the synchronize router architecture, flow f_j obtain the

¹indicator function $1_{\{val\}}$ is equal to 1 if and only if val is true.

² $\delta_0(t) = +\infty$ if $t > 0$, and 0 otherwise.

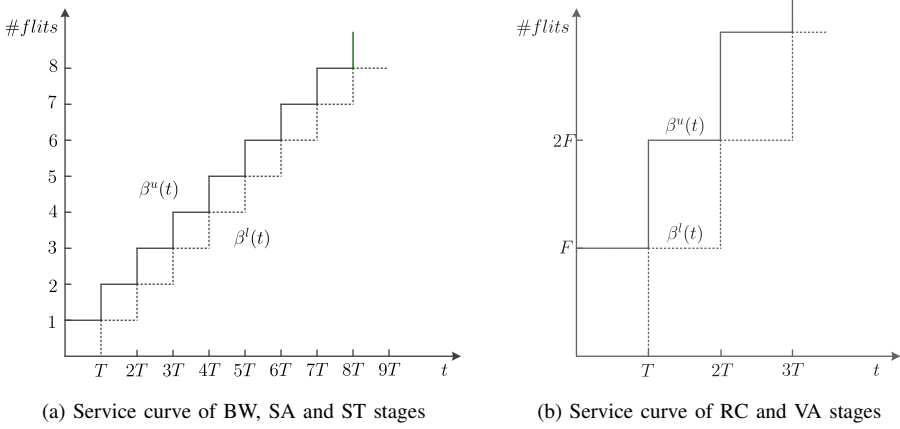


Fig. 3: Service model for each pipeline stages. The solid lines and dotted lines represent the upper service curves and lower service curves, respectively.

total leftover service curve $\langle \beta_{SA,R_i}^{l'}, \beta_{SA,R_i}^{u'} \rangle$. But for an asynchronous architecture, we should take the inference from low-priority flows into consideration. For example, a flit from f_j arriving at SA stage just after a flit from lower priority gotten granted has to stall for a cycle. At this circumstance, the actual service curve obtained by flow f_j is [?]

$$\beta_{SA,R_i,f_j}^l = \max\{0, \beta_{SA,R_i}^{l'} - 1\} \quad (7)$$

where $\beta_{SA,R_i,f_j}^{l'}$ is the leftover service curve calculated with Eq.(3). Similarly, a flow with higher priority than f_j can also be blocked by f_j for a cycle. Thus, denote by $\beta_{SA,R_i,f_j}^{u'}$ the service curve calculated with Eq.(4), the actual upper service curve obtained by flow f_j is [?]

$$\beta_{SA,R_i,f_j}^u = \min\{\beta_{SA,R_i}^u, \beta_{SA,R_i}^{u'} + 1\}. \quad (8)$$

(b) there exists some contention flows with the same priority as f_j . Denote by Θ_{R_i,f_j} the set of contention flows at router R_i with the same priority as f_j , and let N_{R_i,f_j} be the number of flows in Θ_{R_i,f_j} . Since all the flows in Θ_{R_i,f_j} got serviced in Round-Robin order, the service curve provided to f_j is $\langle \lfloor \beta_{SA,R_i}^{l'}/(N_{R_i,f_j}+1) \rfloor, \lceil \beta_{SA,R_i}^{u'}/(N_{R_i,f_j}+1) \rceil \rangle$, where $\lceil \cdot \rceil$ and $\lfloor \cdot \rfloor$ are the ceiling operator and flooring operator. This is slightly different from the conventional continuous time model which is $\langle \beta_{SA,R_i}^{l'}/(N_{R_i,f_j}+1), \beta_{SA,R_i}^{u'}/(N_{R_i,f_j}+1) \rangle$. An example with two flows with the same priority is shown in Fig. 4. After serving by all the flows in Θ_{R_i,f_j} , the leftover service capacity for low priority flows can be obtained by applying Eq.(3) and Eq.(4).

C. Upper Service Curve for Flow Controller

Credit-based flow control introduces cyclic-dependence between the adjacent routers, and leads to the self-blocking within a flow due to the insufficiency of buffer space at the downstream router. Historically, the effect of self-blocking is computed numerically by fixed-point iteration [37] or symbolically analyzed by the transformation from marked dataflow graph [38]. In this paper, we try to tackle the same problem with another solution. This is motivated by [20], where the authors abstract the flow control as a network element (called

flow controller) providing a service curve β_τ (corresponding to the lower service curve in RTC theory), which can be obtained by applying some basic properties of dioid algebra. In this section, we follow the same procedure in [20] to derive the upper service curve for the flow controller. The obtained upper service curve together with the lower service curve derived in [20] enable us to break the control loop caused by flow control and build a comprehensive performance model with RTC. We take flow f_2 as an example to demonstrate this method. The scheduling network of flow f_2 is plotted in Fig. 5, we ignore flow f_4 and the flow control of other flows for simplicity. We assume that, the destination IP core can consume the ejected flits immediately, thus there is no flow controller between the ejection router and destination NI. But, to prevent the buffer overflow, there must be a flow controller between input NI and injection router. We can obtain the upper service curve of flow controller at each router with the following Theorem.

Theorem 1: Suppose the router provides an upper service curve β^u , the buffer size and credit feedback delay are denoted as B and σ . Then the flow controller provides an equivalent upper service curve

$$\beta_\tau^u(t) = \bar{\beta^u} \otimes \delta_\sigma(t) + B$$

where $\bar{\beta^u}$ is the sub-additive closure of β^u [28] and $\delta_\sigma(t) = +\infty$ for $\forall t > \sigma$, otherwise $\delta_\sigma(t) = 0$.

Proof: We take the flow control between R_9 and R_5 in Fig. 5 as an example to proof this theorem. Denote the amount of injected and departed flits at R_5 by time t as $I(t)$ and $D(t)$, and the amount of flits served by R_9 by time t is denoted as $A(t)$. The feedback link can be represented as a network element providing upper service curve $\delta_\sigma(t)$. Next, we apply the basic properties of service curve and dioid algebra to derive the upper service curve this flow controller. We have $I(t) = \min\{A(t), D'(t) + B\}$ by the property of credit-based flow control, where $D' = D \otimes \delta_\sigma$.

Based on property of upper service curve β^u , we have³

$$D(t) \leq I \otimes \beta^u(t).$$

³An alternative definition of upper service curve, see definition 1.6.1 in [28] for more details.



Fig. 4: Service curve of SA stage for two flows with the same priority under Round-Robin scheduling policy. (a) Service capacity of SA stage. (b) Upper and lower service curve provided to each contending flow, corresponding to the solid line and dotted line; the solid green line and dotted red line represent the unrounded upper and lower service curves.

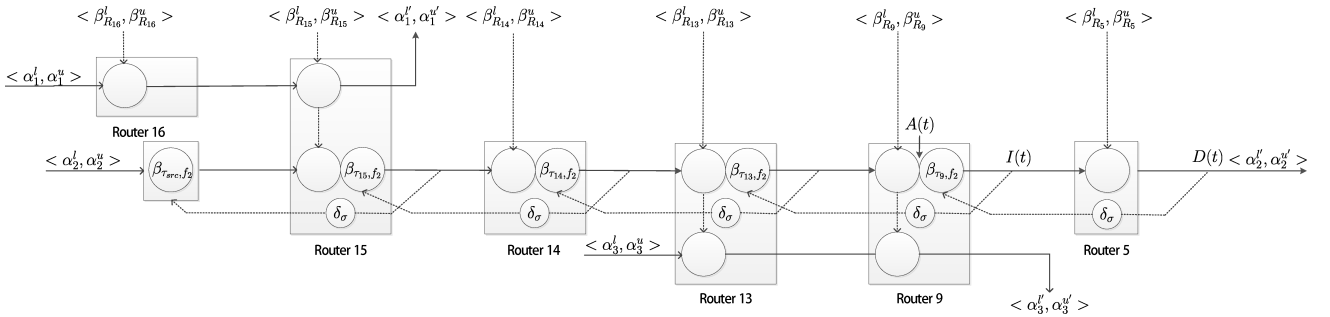


Fig. 5: Scheduling network model for flow \$f_2\$

Bring \$I(t)\$ and \$D'(t)\$ into this equality, we get

$$\begin{aligned} D(t) &\leq I(t) \otimes \beta^u(t) \\ &\leq \min\{A \otimes \beta^u(t), D(t) \otimes \delta_\sigma \otimes \beta^u(t) + B\}. \end{aligned}$$

By applying Theorem 4.31 in [28], we have

$$D \leq A \otimes \beta^u \otimes \overline{\beta^u \otimes \delta_\sigma + B}.$$

Thus,

$$\begin{aligned} I &= \min\{A, D + B\} \\ &\leq \min\{A, D \otimes \delta_\sigma + B\} \\ &\leq \min\{A, A \otimes \beta^u \otimes \overline{\beta^u \otimes \delta_\sigma + B} \otimes \delta_\sigma + B\} \\ &= \min\{A \otimes \delta_\sigma, A \otimes (\beta^u \otimes \delta_\sigma + B) \otimes \overline{\delta_\sigma \otimes \beta^u + B}\} \\ &= \min\{A \otimes \delta_\sigma, A \otimes \overline{\delta_\sigma \otimes \beta^u + B}\} \\ &= A \otimes \min\{\delta_\sigma, \overline{\beta^u \otimes \delta_\sigma + B}\} \\ &= A \otimes \overline{\beta^u \otimes \delta_\sigma + B}. \end{aligned}$$

which implies that, the flow controller has an equivalent upper service curve \$\overline{\beta^u \otimes \delta_\sigma + B}\$. ■

Theorem 1 derives the upper service curve of a single flow controller, and we can get the service curves of all the flow controllers along the router chain of all the flows by applying Theorem 1 iteratively. As shown in Fig. 5, the service curve of downstream routers can affect the service curve of flow

controller at upstream. Hence, we should compute the service curves of flow controller from ejection router to injection router. Take flow \$f_2\$ as an example, we should first derive the service curves of \$f_2\$ obtained at each router with the method provided in Subsection IV-B. Service curve obtained at Router \$R_{15}\$ to flow \$f_2\$ can be derived by applying Eq.(3) and Eq.(4), since \$f_2\$ is a lower priority flow at \$R_{15}\$. Router \$R_{13}\$, \$R_9\$ and \$R_5\$ provide all their service capacity to \$f_2\$ because \$f_2\$ is the highest priority flow at these routers. Then, the service curve of flow controller at router \$R_9\$ can be obtained by applying Theorem 1, which is \$<\beta_{\tau_9}^l, \beta_{\tau_9}^u>\$. By applying the concatenation theorem, we can obtain the equivalent service curve of router \$R_9\$ are \$<\beta_{R_9}^l \otimes \beta_{\tau_9}^l, \beta_{R_9}^u \otimes \beta_{\tau_9}^u>\$. Follow the same procedure, we can get the service curve of flow controller at router \$R_{13}\$, \$R_{14}\$, \$R_{15}\$ and the source NI that connected to \$R_{15}\$ iteratively.

D. Collapsible Sub-Path

To this end, we have build the traffic model, router model and flow control model in the previous subsections. Before giving the latency analysis algorithm algorithm, we first consider the follow scenario. Flow \$f_2\$ and \$f_3\$ in Fig. 1 contend the output link at both router \$R_{13}\$ and \$R_9\$. Suppose \$P_2 > P_3\$ and denote by \$B_{R_9, f_2}\$ the buffer size of router \$R_9\$ allocated to flow \$f_2\$, \$<\beta_{R_{13}, f_2}^l, \beta_{R_{13}, f_2}^u>\$ and \$<\beta_{R_9, f_2}^l, \beta_{R_9, f_2}^u>\$ the service curve provided to flow \$f_2\$ by router \$R_{13}\$ and \$R_9\$,

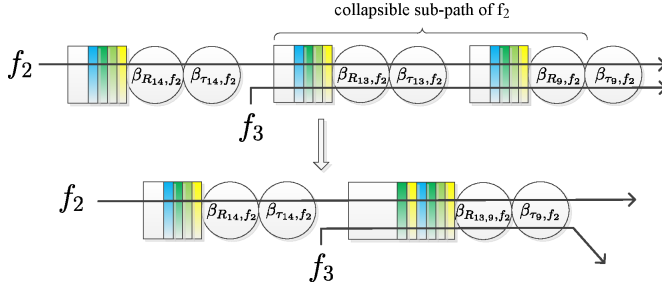


Fig. 6: Collapsible sub-path of f_2 . Since the flow control between R_{13} and R_9 can be ignored, they are replaced by a single virtual router $R_{13,9}$.

$\langle \beta_{\tau_{13}, f_2}^l, \beta_{\tau_{13}, f_2}^u \rangle$ the service curve for flow controller of router R_{13} , $\langle \alpha_{R_{13}, f_2}^l, \alpha_{R_{13}, f_2}^u \rangle$ and $\langle \alpha_{R_{13}, f_3}^l, \alpha_{R_{13}, f_3}^u \rangle$ the arrival curve of f_2 and f_3 at router R_{13} . The question is: when B_{R_9, f_2} is sufficiently large so that $\beta_{R_{13}, f_2}^l \otimes \beta_{\tau_{13}, f_2}^l = \beta_{R_{13}, f_2}^l$ and $\beta_{R_{13}, f_2}^u \otimes \beta_{\tau_{13}, f_2}^u = \beta_{R_{13}, f_2}^u$, how to derive the leftover service curve for f_3 at R_{13} and R_9 , and obtain a tight performance bound of f_3 efficiently?

An intuitive solution is: Firstly, obtaining the leftover service curve of R_{13} by applying Eq.(3) and Eq.(4); Secondly, deriving the output arrival curve $\langle \alpha_{R_9, f_2}^l, \alpha_{R_9, f_2}^u \rangle$ of f_2 by applying Eq.(1) and Eq.(2); Thirdly, the leftover service curve of R_9 can be easily obtained by applying Eq.(3) and Eq.(4); And finally, the leftover service curve for f_3 at R_{13} and R_9 can be easily obtained by concatenating these two service curves. Another solution is: we can substitute R_{13} and R_9 by a virtual router $R_{13,9}$ providing service curve $\langle \beta_{R_{13}, f_2}^l \otimes \beta_{R_{13}, f_2}^l, \beta_{R_{13}, f_2}^u \otimes \beta_{R_{13}, f_2}^u \rangle$, since B_{R_9, f_2} is sufficiently large and the flow control between R_{13} and R_9 can be ignored, as shown in Fig. 6. Then, the service curve of f_3 obtained at R_{13} and R_9 can be directly obtained by applying Eq.(3) and Eq.(4). Compared with previous router-by-router calculation method, it eliminates the calculation of intermediate arrival curve, and compute the equivalent service curve by just invoke Eq.(3) and Eq.(4) once, which is calculation efficient. We formalize this observation and propose the concept of Collapsible Sub-Path (CSP).

Definition 3 (Collapsible Sub-Path): The collapsible sub-path of flow f , denoted by $CSP(f)$, is a sub-path of f satisfying the follow conditions:

- 1) all the routers R_i on this sub-path, except the last one, satisfy $\beta_{R_i, f}^l \otimes \beta_{\tau_i, f}^l = \beta_{R_i, f}^l$ and $\beta_{R_i, f}^u \otimes \beta_{\tau_i, f}^u = \beta_{R_i, f}^u$.
- 2) $CSP(f)$ is also a sub-path of all the flows in Ω_f , where Ω_f is the set of contention flows with lower priorities on this sub-path.

For the high-priority flows, the process of calculating the end-to-end equivalent service curve is also a collapsing process. But, to compute the leftover service curve for low-priority flows at some routers, we have to know the arrival curve of high-priority flows at these routers. As implied previously, instead of the router-by-router calculation, we can leverage the concept of CSP and replace all the routers on $CSP(f)$ with a single virtual router providing service curve $\otimes_{R_i \in CSP(f)} \beta_{R_i, f}^l, \otimes_{R_i \in CSP(f)} \beta_{R_i, f}^u \rangle$. For a CSP with n

($n \geq 2$) routers, this method reduces $n - 1$ times calculation of arrival curve and leftover service curve. The leftover service curve calculation is greatly simplified, and the accuracy of performance bound is also improved due to the well-known “Pay-Burst-Only-Once” phenomenon in DNC theory [28].

E. End-to-End Latency

After obtained the traffic model, router model and flow control model, compute the end-to-end latency is still a non-trivial task. The follow four aspects should be considered carefully: (1) We should always compute the end-to-end latency by collapsing all the CSP to a single virtual node, as the hop-by-hop computation will lead to a looser bound; (2) In the fixed-priority flit-level preemptive NoC, only the leftover service curve can be used by the low priority flows, thus, the computation process must start from high-priority flows to low-priority flows; (3) Before computing the leftover service curve for lower priority flows, we must ensure that all the higher priority flows has been served; (4) The computed service curve for flow controller can only be applicable for specific flow, and we should compute these curves for each flows. Keeping these four aspects in mind, we propose the performance evaluation algorithm, as shown in Algorithm 1.

Suppose the entire NoC is represented as a directional topology graph $G : V \times E$, where V and E represent the set of routers and links, respectively. For each link $e_{i,j} \in E$ represent there is a physical channel between router R_i and router R_j , $e_{i,j} \neq e_{j,i}$ since the topology graph is a directional graph. The set of all the flows in the network is denoted as \mathcal{F} , and each flow $f_i \in \mathcal{F}$ has a fixed-priority P_i . The set of routers a flow f_i traversed is denoted as \mathcal{R}_i , and the set of links a flow f_i traversed is denoted as Γ_i . If there exists interference between flow f_i and f_j , then $\Gamma_i \wedge \Gamma_j \neq \emptyset$ and the set of contention routers is $\mathcal{R}_i \wedge \mathcal{R}_j$. Denote by $\langle \alpha_{f_i}^l, \alpha_{f_i}^u \rangle$ the arrival curve of flow f_i at the ingress port. Suppose the arrival curve of f_i at router R_j is $\langle \alpha_{R_j, f_i}^l, \alpha_{R_j, f_i}^u \rangle$, and the leftover service curve of SA stage at router R_j is denoted as $\langle \beta_{SA, R_j}^l, \beta_{SA, R_j}^u \rangle$ (Initially, $\beta_{SA, R_j}^l = \beta_{SA, R_j}^u$ and $\beta_{SA, R_j}^u = \beta_{SA, R_j}^u$). The path of flow f_i is started from ingress router (denoted by $start_i$) to egress router (started by end_i). For all the router R_j along the path of flow f_i , denote by the contention flows with the same priority as f_i as Θ_{R_j, f_i} , the set with lower priority flow as Ω_{R_j, f_i} , and the buffer size as B_{R_j, f_i} . In addition, let N_{R_j, f_i} and N_{f_i} be the number of flows in Θ_{R_j, f_i} and the number of routers that f_i traversed.

The proposed algorithm calculates the end-to-end latency from high-priority flows to low-priority flows, and for each iteration, performs the following four steps: (1) Calculating the service curve provided by router (line 4 to line 10) and flow controller (line 11 to line 12); (2) Identifying and collapsing all the CSP on the path of a flow to improve the analyzing accuracy (line 14); (3) Computing the worst-case end-to-end latency (line 15); (4) Calculating the leftover service curve for low-priority flows (line 16 to line 32). We also need to emphasize that, the leftover service curve for lower priority flows should compute after all the service curve of higher priority flows have been calculated, as implied by

Algorithm 1 End-to-End Latency Analysis Algorithm

Require: Scheduling Network
Ensure: Worst-case End-to-End Latency for all the flows

- 1: **for** each flow $f_i \in \mathcal{F}$ with priority order **do**
- 2: $\beta_\tau^l = \delta_0(t); \beta_\tau^u = \delta_0(t);$
- 3: **for** each router $R_j \in \mathcal{R}_i$ from end_i to $start_i$ **do**
- 4: **if** $\Theta_{R_j, f_i} \neq \emptyset$ **then**
- 5: $\beta_{R_j, f_i}^l = \beta_{BW}^l \otimes \beta_{RC}^l \otimes \beta_{VA}^l \otimes \lfloor \frac{\beta_{SA, R_j}^{l'}}{N_{R_j, f_i} + 1} \rfloor \otimes \beta_{ST}^l;$
- 6: $\beta_{R_j, f_i}^u = \beta_{BW}^u \otimes \beta_{RC}^u \otimes \beta_{VA}^u \otimes \lceil \frac{\beta_{SA, R_j}^{u'}}{N_{R_j, f_i} + 1} \rceil \otimes \beta_{ST}^u;$
- 7: **else**
- 8: $\beta_{R_j, f_i}^l = \beta_{BW}^l \otimes \beta_{RC}^l \otimes \beta_{VA}^l \otimes \beta_{SA, R_j}^{l'} \otimes \beta_{ST}^l;$
- 9: $\beta_{R_j, f_i}^u = \beta_{BW}^u \otimes \beta_{RC}^u \otimes \beta_{VA}^u \otimes \beta_{SA, R_j}^{u'} \otimes \beta_{ST}^u;$
- 10: **end if**
- 11: $\beta_{\tau_j, f_i}^l(t) = \beta_\tau^l; \beta_\tau^l = \beta_{R_j, f_i}^l \otimes \beta_\tau^l \otimes \delta_\sigma(t) + B_{R_j, f_i};$
- 12: $\beta_{\tau_j, f_i}^u(t) = \beta_\tau^u; \beta_\tau^u = \beta_{R_j, f_i}^u \otimes \beta_\tau^u \otimes \delta_\sigma(t) + B_{R_j, f_i};$
- 13: **end for**
- 14: Collapse $CSP(f_i)$ and update $\Theta_{R_j, .}, \Omega_{R_j, .}$ and \mathcal{R}_i ;
- 15: $Delay(f_i) = H(\alpha_{f_i}^u, \bigotimes_{R_k \in \mathcal{R}_{f_i}} (\beta_{R_k, f_i}^l \otimes \beta_{\tau_k, f_i}^l));$
- 16: $\beta_{f_i}^l = \delta_0(t); \beta_{f_i}^u = \delta_0(t);$
- 17: **for** For $\forall R_j \in \mathcal{R}_{f_i}$ from $start_i$ to end_i **do**
- 18: $\beta^l = \beta_{f_i}^l \otimes \beta_{BW}^l \otimes \beta_{RC}^l \otimes \beta_{VA}^l;$
- 19: $\beta^u = \beta_{f_i}^u \otimes \beta_{BW}^u \otimes \beta_{RC}^u \otimes \beta_{VA}^u;$
- 20: $\alpha_{R_j, f_i}^l = \min\{(\alpha_{f_i}^l \otimes \beta^u) \otimes \beta^l, \beta^l\};$
- 21: $\alpha_{R_j, f_i}^u = \min\{(\alpha_{f_i}^u \otimes \beta^u) \otimes \beta^l, \beta^u\};$
- 22: $\beta_{f_i}^l = \beta_{f_i}^l \otimes \beta_{R_j, f_i}^l \otimes \beta_{R_j, f_i}^l;$
- 23: $\beta_{f_i}^u = \beta_{f_i}^u \otimes \beta_{R_j, f_i}^u \otimes \beta_{R_j, f_i}^u;$
- 24: **if** $\Omega_{R_j, f_i} \neq \emptyset$ **then**
- 25: **if** delay of $\forall f_k \in \Theta_{R_j, f_i}$ has been calculated **then**
- 26: $\alpha_{R_j, f_i}^l = \alpha_{R_j, f_i}^l + \sum_{f_k \in \Theta_{R_j, f_i}} \alpha_{R_j, f_k}^l;$
- 27: $\alpha_{R_j, f_i}^u = \alpha_{R_j, f_i}^u + \sum_{f_k \in \Theta_{R_j, f_i}} \alpha_{R_j, f_k}^u;$
- 28: **end if**
- 29: $\beta_{SA, R_j}^{l'} = (\beta_{SA, R_j}^{l'} - \alpha_{R_j, f_i}^u) \bar{\otimes} 0;$
- 30: $\beta_{SA, R_j}^{u'} = \max\{(\beta_{SA, R_j}^{u'} - \alpha_{R_j, f_i}^l) \bar{\otimes} 0, 0\};$
- 31: **end if**
- 32: **end for**
- 33: **end for**

line 25 in Algorithm 1. The overall algorithm has two-level embedded loops, and the computation complexity for this algorithm is $O(pN)$, where N and p is the number of flows and the hop count of each flow. This algorithm is of pseudo-polynomial complexity due to the computation complexity of algorithmic min-plus convolution and sub-additive closure [39]. This algorithm can be easily integrated into the RTC toolbox [33] to compute the end-to-end latency automatically.

F. Buffer Optimization

The priority-aware wormhole-switched NoC [7] requires the same amount of VC as the priorities to prevent priority inversion [11], which refers to the blocking of high-priority flows when the low-priority flows occupy all the VCs. To reduce the buffer area and power consumption, priority sharing [40] and buffer optimization [15] techniques are proposed.

However, the two backlog bounds derived in [15] is the minimum buffer size that does not trigger the flow control, which can be further reduced as long as the constraint of deadline is not be violated. Suppose the application has been mapped onto the NoC, and each flow f_i has been assigned to their corresponding priority P_i and deadline D_i . Following the same notations as Algorithm 1, we propose the buffer optimization algorithm to further reduce the buffer size, as shown in Algorithm 2. It tries to optimize the buffer size for each flow from high-priority to low-priority gradually. For each iteration, it performs the following four steps: (1) Calculating the service curve provided by router (line 3 to line 9); (2) Calculate the minimum buffer size that can avoid flow control (line 10 to line 13); (3) Reduce the initial buffer size gradually as long as the constraint of deadline is not violated (line 15 to line 26); (4) Calculating the leftover service curve for low-priority flows (line 27 to line 43).

Decreasing the buffer size increases the possibility of flow control, which prevents the flits progressing in the network and leads to a larger end-to-end latency. The amount of cycles that a packet can be stalled in the network without violating the deadline is referred to ‘slack’. We can reduce the buffer size as long as slack is greater than zero. Our buffer optimization algorithm can be used to reduce the router area and power consumption. But, there is significant difference between the DNC based slack optimization in [41] and our method. In [41], the energy optimization is carried out with Dynamic Voltage and Frequency Scaling (DVFS), they minimize the energy consumption by adjusting the voltage and frequency for the fixed configuration and deadline. In contrast, our method try to optimize the buffer size under the deadline constraint, and the buffer reduction directly leads to the area and power saving. In addition, our algorithm can be used in conjunction with the priority sharing techniques [40] to optimize the buffer size of priority-aware wormhole-switched NoC .

This algorithm can be implemented in RTC toolbox [33] to optimize the buffer size automatically. The entire computation complexity is $O(pN)$, where N and p are the number of flows and the number of routers along the path. This complexity is pseudo-polynomial due to the end-to-end latency calculation. We can also halt the optimization when the buffer budget are met to reduce the computation procedure. A significant difference with Algorithm 1 is that, this algorithm does not identify and collapse the CSP, because the reduction of buffer size introduces flow control between adjacent routers. To this end, both the proposed algorithm 1 and algorithm 2 assume the NoC is synchronous. But we claim that, our method can also be easily extended to support asynchronous NoC. For an asynchronous NoC, a low-priority flow might blocking a high-priority flow at most 1 cycle. This is achieved by simply applying Eq.(7) and Eq.(8) on the leftover service curve of line 29 and line 30 in algorithm 1 and algorithm 2. In addition, the initial value of $\langle \beta_{SA, R_j}^{l'}, \beta_{SA, R_j}^{u'} \rangle$ should be processed with Eq.(7) and Eq.(8), too.

V. EXPERIMENTS

In this section, we validate the correctness and tightness of our calculated performance bounds by comparison with other

Algorithm 2 Buffer Optimization Algorithm

Require: Scheduling Network and Deadline for all the flows
Ensure: Optimized Buffer Size

```

1: for each flow  $f_i \in \mathcal{F}$  with priority order do
2:   for each router  $R_j \in \mathcal{R}_i$  do
3:     if  $\Theta_{R_j, f_i} \neq \emptyset$  then
4:        $\beta_{R_j, f_i}^l = \beta_{BW}^l \otimes \beta_{RC}^l \otimes \beta_{VA}^l \otimes \lfloor \frac{\beta_{SA, R_j}^{l'}}{N_{R_j, f_i} + 1} \rfloor \otimes \beta_{ST}^l$ ;
5:        $\beta_{R_j, f_i}^u = \beta_{BW}^u \otimes \beta_{RC}^u \otimes \beta_{VA}^u \otimes \lceil \frac{\beta_{SA, R_j}^{u'}}{N_{R_j, f_i} + 1} \rceil \otimes \beta_{ST}^u$ ;
6:     else
7:        $\beta_{R_j, f_i}^l = \beta_{BW}^l \otimes \beta_{RC}^l \otimes \beta_{VA}^l \otimes \beta_{SA, R_j}^{l'} \otimes \beta_{ST}^l$ ;
8:        $\beta_{R_j, f_i}^u = \beta_{BW}^u \otimes \beta_{RC}^u \otimes \beta_{VA}^u \otimes \beta_{SA, R_j}^{u'} \otimes \beta_{ST}^u$ ;
9:     end if
10:     $B^l = \inf\{B | \beta_{R_j, f_i}^l \otimes \overline{\beta_{R_j, f_i}^l \otimes \delta_\sigma(t) + B} \geq \beta_{R_j, f_i}^l\}$ ;
11:     $B^u = \inf\{B | \beta_{R_j, f_i}^u \otimes \overline{\beta_{R_j, f_i}^u \otimes \delta_\sigma(t) + B} \geq \beta_{R_j, f_i}^u\}$ ;
12:     $B_{R_j, f_i} = \max\{B^l, B^u\}$ ;
13:     $\beta_{\tau_j, f_i}^l = \delta_0(t); \beta_{\tau_j, f_i}^u = \delta_0(t)$ ;
14:  end for
15:  for each router  $R_j \in \mathcal{R}_i$  from  $end_i$  to  $start_i$  do
16:     $Delay(f_i) = H(\alpha_{f_i}^u, \bigotimes_{R_k \in \mathcal{R}_{f_i}} (\beta_{R_k, f_i}^l \otimes \beta_{\tau_k, f_i}^l))$ ;
17:    while  $Delay(f_i) \leq D_i$  and  $B_{R_j, f_i} > 1$  do
18:       $B_{R_j, f_i} = B_{R_j, f_i} - 1$ ;
19:      Recalculate  $\beta_{\tau_k, f_i}^l$  for all  $R_k$  from  $R_j$  to  $start_i$ ;
20:       $Delay(f_i) = H(\alpha_{f_i}^u, \bigotimes_{R_k \in \mathcal{R}_{f_i}} (\beta_{R_k, f_i}^l \otimes \beta_{\tau_k, f_i}^l))$ ;
21:    end while
22:    if  $Delay(f_i) > D_i$  then
23:       $B_{R_j, f_i} = B_{R_j, f_i} + 1$ ;
24:      Update  $\langle \beta_{\tau_j, f_i}^l, \beta_{\tau_j, f_i}^u \rangle$ ;
25:    end if
26:  end for
27:   $\beta_{f_i}^l = \delta_0(t); \beta_{f_i}^u = \delta_0(t)$ ;
28:  for For  $\forall R_j \in \mathcal{R}_{f_i}$  from  $start_i$  to  $end_i$  do
29:     $\beta^l = \beta_{f_i}^l \otimes \beta_{BW}^l \otimes \beta_{RC}^l \otimes \beta_{VA}^l$ ;
30:     $\beta^u = \beta_{f_i}^u \otimes \beta_{BW}^u \otimes \beta_{RC}^u \otimes \beta_{VA}^u$ ;
31:     $\alpha_{R_j, f_i}^l = \min\{(\alpha_{f_i}^l \otimes \beta^u) \otimes \beta^l, \beta^l\}$ ;
32:     $\alpha_{R_j, f_i}^u = \min\{(\alpha_{f_i}^u \otimes \beta^u) \otimes \beta^l, \beta^u\}$ ;
33:     $\beta_{f_i}^l = \beta_{f_i}^l \otimes \beta_{R_j, f_i}^l \otimes \beta_{\tau_j, f_i}^l$ ;
34:     $\beta_{f_i}^u = \beta_{f_i}^u \otimes \beta_{R_j, f_i}^u \otimes \beta_{\tau_j, f_i}^u$ ;
35:    if  $\Omega_{R_j, f_i} \neq \emptyset$  then
36:      if delay of  $\forall f_k \in \Theta_{R_j, f_i}$  has been calculated then
37:         $\alpha_{R_j, f_i}^l = \alpha_{R_j, f_i}^l + \sum_{f_k \in \Theta_{R_j, f_i}} \alpha_{R_j, f_k}^l$ ;
38:         $\alpha_{R_j, f_i}^u = \alpha_{R_j, f_i}^u + \sum_{f_k \in \Theta_{R_j, f_i}} \alpha_{R_j, f_k}^u$ ;
39:      end if
40:       $\beta_{SA, R_j}^{l'} = (\beta_{SA, R_j}^{l'} - \alpha_{R_j, f_i}^u) \bar{\otimes} 0$ ;
41:       $\beta_{SA, R_j}^{u'} = \max\{(\beta_{SA, R_j}^{u'} - \alpha_{R_j, f_i}^l) \bar{\otimes} 0, 0\}$ ;
42:    end if
43:  end for
44: end for
```

analytical methods and simulation. Several analytical methods exist for the delay analysis of priority-aware NoC, examples include contention tree model [26], lumped link model [11], dependency graph model [8], FLA [7], LLA [14] and DNC [16], etc. There are also extensive research on the buffer sizing of priority-aware NoC, representative works include shaping delay analysis [42] and LLBA [15]. In addition, the DNC model in [16] can also be deployed to calculate the buffer bound. Among all these analytical methods, LLA and DNC based model outperform the others when the tightness of delay and backlog bound are considered. Thus, we will perform detailed comparison with LLA and DNC in this section. We perform the comparison on a set of periodical traffic, due to the restriction of LLA method. Denote by the packet length of flow f_i is F_i (in flits) and the injection period is I_i . Packets from the same flow has the same length, but packets of different flows can be of different lengths. The detailed comparison with LLA and DNC are performed in subsection V-A and subsection V-B, respectively.

A. Comparison with Link Level Analysis

To ease the analysis, LLA supposes the number of bits in a flit is the same as the physical channel width, and the latency of a flit traverses a router is 1 cycle. Under these assumptions, the traversing time of a packet with F_i flits without contention, i.e. L_i , is equal to F_i . To compare with our method, we should specialize the standard 5 stages wormhole router to a single cycle router, this is achieved by letting the latency of BW, RC, VA and ST stage be zero. Thus, the service curve of entire router is the same as the service curve provided by the SA stage, which is $\langle \beta_{SA, R_i}^l, \beta_{SA, R_i}^u \rangle$. The network topology and flows are shown in Fig. 1. There are four flows (i.e. f_1, f_2, f_3 and f_4) in the network, with different priority $P_4 > P_1 > P_2 > P_3$. The LLA method does not consider the self-blocking caused by flow control. Thus, we set the credit feedback delay $\sigma = 0$ cycle in our model for a fair comparison. Next, we compare the end-to-end latency and buffer requirement computed with LLA and RTC.

1) End-to-End Latency: For this scenario, we suppose the VC buffer is large enough so that we can ignore the back-pressure caused by flow control and directly apply LLA for the latency analysis. We examine the end-to-end latency of the four flows in Fig. 1 under different packet length L_i and injection period I_i , the calculated result is shown in Table I. Each element in the table is a quaternion, corresponding to the worst-case latency of f_1, f_2, f_3 and f_4 . The blanking items in the table corresponding to the scenarios that the worst-case latency of a flow is greater than its injection period, which is unable to be analyzed with LLA [14]. In contrast, the RTC method is able to tackle these circumstance and give the worst-case latency. The RTC result is obtained by collapsing the CSP of f_2 (i.e. R_{13} and R_9).

As shown in the table I, for the given configuration, RTC result is as tight as that of LLA except for the scenarios that the worst-case latency of a flow is equal to the injection period. This is because the RTC is stateless algebra approach, and ignored some detailed information about the system [?]. We

TABLE I: Delay comparison with link level analysis

I_i	$L_i = 1$		$L_i = 2$		$L_i = 4$	
	RTC	LLA	RTC	LLA	RTC	LLA
3	7,8,8,4	—	—	—	—	—
5	6,6,6,4	—	9,10,12,5	—	—	—
6	5,6,6,4	5,6,5,4	9,8,9,5	—	—	—
7	5,6,5,4	5,6,5,4	7,8,9,5	—	—	—
8	5,6,5,4	5,6,5,4	7,8,9,5	7,8,7,5	—	—
9	5,6,5,4	5,6,5,4	7,8,7,5	7,8,7,5	15,16,19,7	—
11	5,6,5,4	5,6,5,4	7,8,7,5	7,8,7,5	15,12,15,7	—
13	5,6,5,4	5,6,5,4	7,8,7,5	7,8,7,5	11,12,15,7	—
15	5,6,5,4	5,6,5,4	7,8,7,5	7,8,7,5	11,12,11,7	11,12,11,7
17	5,6,5,4	5,6,5,4	7,8,7,5	7,8,7,5	11,12,11,7	11,12,11,7

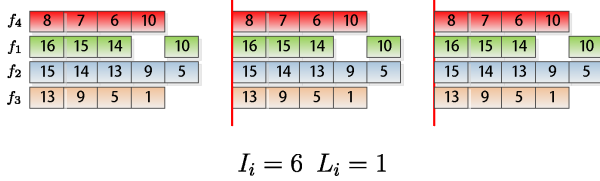


Fig. 7: Time line graph of the four flows in Fig. 1. Each block represents a router, and the color of the block means which flow are occupying the router at this time instance.

also found that, both the LLA and RTC overestimate the worst-case latency bound. To demonstrate this, let $L_i = 1$ flit, $I_i = 6$ cycle, we plot the time line graph for the four flows in Fig. 1, as shown in Fig. 7. From this figure, we can find that, the worst-case latency of these four flows computed with LLA (5,6,5,4) and RTC (5,6,6,4) are looser than the actual latency, which are 5 cycle, 5 cycle, 4 cycle, 4 cycle, respectively.

2) *Buffer Optimization*: The proposed LLBA method [15] can give the required buffer size of each VC to prevent flow control, this buffer size can be further reduced as long as the deadline is not violated. In this section, we try to demonstrate that, the RTC method can optimize the buffer size further by taking the flow control into consideration. Suppose the injection period $I_i = 20$ and packet size $F_i = 4$ ($i = 1, 2, 3, 4$), following the same configuration with the previous subsection, we can get the end-to-end latency for the four flows, which are 11, 12, 11 and 7, respectively. We can also get the buffer size reserved at each router with LLBA method, which are (1, 1, 1, 4), (1, 1, 1, 1, 1), (4, 4, 1, 1) and (1, 1, 1, 1), respectively. We change the deadline constraint from 15 cycle to 27 cycle, and compute the required buffer size for each flow with our buffer optimization algorithm, the result is shown in Table II.

B. Comparison with Network Calculus and Simulation

In this subsection, we present the numerical results to demonstrate the tightness and improvement of our method over DNC method proposed in [16]. The correctness of our latency model and buffer optimization algorithm is verified by simulation. We modified the switch allocator of a modular open source NoC simulator, Heterogenous Networks-on-Chip (HNoCs) [43], to support fixed-priority scheduling, and collect the maximal end-to-end packet delay at each destination IP core. We can obtain the arrival curve according to the method

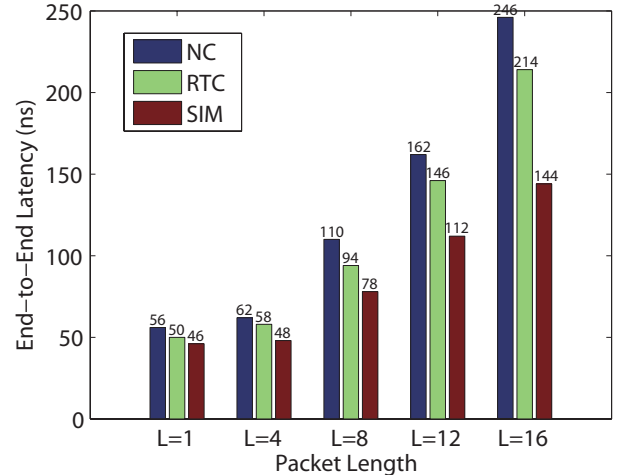


Fig. 8: Comparison with network calculus and simulation

introduced in subsection IV-A. In [16], the authors derived the service curve for each contention flow at the same input router. But, these service curves can only be used to derive the latency of injection router, for the service curve of each flow at subsequent router, the service curve should be computed with the same procedure as [20]. We set the clock cycle as $T = 2\text{ns}$, flit injection rate as 0.1 flit/cycle, buffer depth as $B = 4$ flits, credit feedback delay $\sigma = 0$ cycle, and change the packet length from 1 flit to 16 flits. The priority of each flow in Fig. 1 is denoted as P_i ($i = 1, 2, 3, 4$), and we assume $P_4 = P_1 > P_2 > P_3$. The simulation results and numerical results of f_3 is plotted in Fig. 8. By comparison, we find that RTC can derive a much tighter latency bound compared with DNC, and the difference becomes larger when we increase the packet length.

Next, we explain the reason why our method outperform the DNC based method proposed in [16]. As implied by Theorem 1.72 in [28], the maximal service curve of current router can limit the arrival curve of next router, which leads to a tighter leftover service curve at next router for the other flows. To demonstrate this, let $B = 4$ flits, $L = 4$ flits, $\sigma = 0$ cycle and $T = 2\text{ns}$, we obtained the calculated service curve for flow f_2 both with DNC and RTC, as shown in Fig. 9. The numerical calculation was carried out with RTC toolbox. From Fig. 9, we find that, the calculated service curve with RTC is much ‘better’ than DNC, which explains why the RTC can produce better results.

As has shown in previous subsections, the DNC based method [16] can handle some circumstances that FLA and LLA can not be applied. This motivate us to optimize the buffer size of NoC with our method. Let the flit injection rate be 0.1 flit/cycle, feedback delay $\sigma = 0$ cycle, packet length $L = 16$ flits and change the VC buffer depth from 4 flits to 10 flits, we compare the theoretical bound computed with DNC and our method, as shown in Fig. 10. It clear that, our method outperform the DNC based method, because it gives much tight bound for both f_2 and f_3 . Further, if we set the deadline of f_2 and f_3 to 150ns, with our method, we can

TABLE II: buffer requirement comparison

(D_1, D_2, D_3, D_4)	f_1 $(B_{16}, B_{15}, B_{14}, B_{10})$	f_2 $(B_{15}, B_{14}, B_{13}, B_9, B_5)$	f_3 (B_{13}, B_9, B_5, B_1)	f_4 (B_8, B_7, B_6, B_{10})	Required Buffer Size
(15,15,15,15)	(1,1,1,2)	(2,1,1,1)	(4,4,1,1)	(1,1,1,1)	25
(17,17,17,17)	(1,1,1,2)	(2,1,1,1)	(3,3,1,1)	(1,1,1,1)	23
(19,19,19,19)	(1,1,1,2)	(2,1,1,1)	(2,2,1,1)	(1,1,1,1)	22
(21,21,21,21)	(1,1,1,2)	(1,1,1,1)	(2,2,1,1)	(1,1,1,1)	20
(23,23,23,23)	(1,1,1,1)	(1,1,1,1)	(2,2,1,1)	(1,1,1,1)	19
(25,25,25,25)	(1,1,1,1)	(1,1,1,1)	(2,2,1,1)	(1,1,1,1)	19
(27,27,27,27)	(1,1,1,1)	(1,1,1,1)	(1,1,1,1)	(1,1,1,1)	17

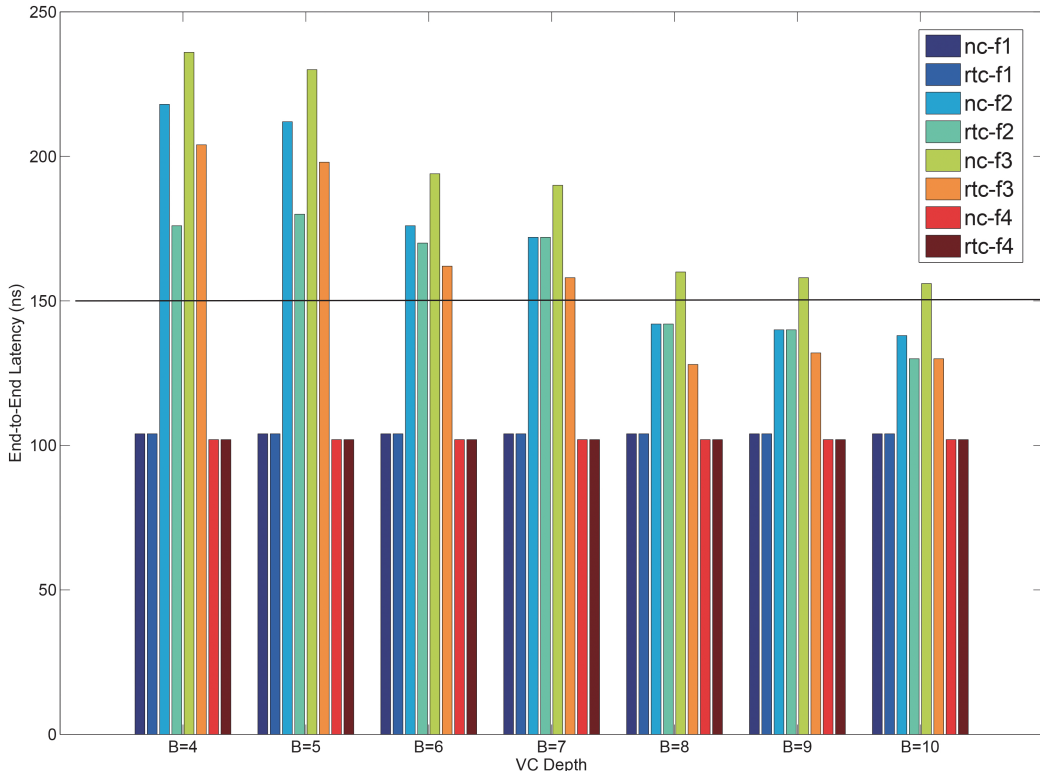


Fig. 10: End-to-end flows with different buffer size

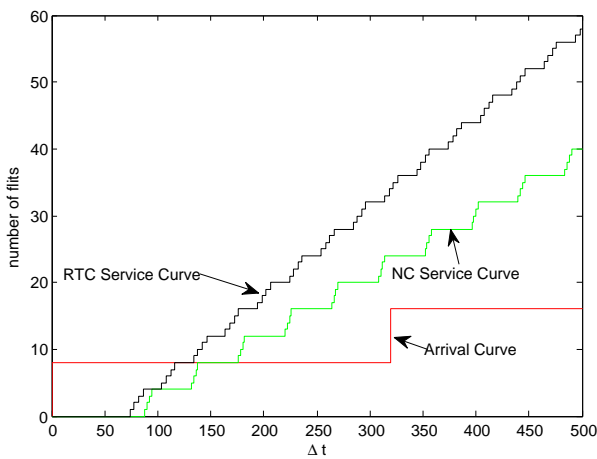


Fig. 9: Comparison of service curve computed with real-time calculus and network calculus

found that $B = 8$ flits is sufficient enough to guarantee the delay bound. While the DNC based estimation is larger than 10 flits. We also observed from Fig. 10 that, the high priority flows (i.e. f_1 and f_4) are very insensitive to the buffer depths, which motivate us to allocate small buffers for these flows to reduce the area and power cost. We also observed that, for the priority-aware NoC, the lower priorities, the higher blocking ratios, thus leading to a larger buffer requirement.

VI. CONCLUSION

The priority-aware wormhole-switched NoC is a promising platform for the on-chip real-time communication if the worst-case performance can be accurately analyzed and guaranteed. Simulation is not competent for this purpose because it is difficult to cover all the corner cases. In this paper, we propose an RTC based analytical model to achieve this goal. We first build the traffic model and service model for this NoC, and propose a novel method to derive the upper service curve of window flow control. Then, based on the proposed RTC model, we proposed an end-to-end latency analyzing

algorithm and a buffer optimization algorithm. The latency analyzing algorithm can be implemented in RTC toolbox to compute the end-to-end latency for each flow automatically, to verify whether all these flows meet their deadline under this configuration. To improve the calculated delay bound, we proposed the concept of collapsible sub-path. The proposed buffer optimization algorithm can optimize the buffer size iteratively, from high-priority flows to low-priority flows. It can also be implemented with RTC toolbox to perform the buffer optimization automatically under the constraint of deadline. Experiment results demonstrate that, our method outperforms the conventional analytical methods, e.g. LLA and DNC, when the tightness of performance bound are considered. Our results can also be applied to the mapping, routing and power optimization of NoC.

ACKNOWLEDGEMENT

The authors would thank the reviewers for their suggestions and comments, and all the experiments are carried out at Integrated Microsystem Lab (IML) of McGill University. This research is supported by High Technology Research and Development Program of China (Grant No. 2012AA012201, 2012AA011902).

REFERENCES

- [1] E. Bolotin, Z. Guz, I. Cidon, R. Ginosar, and A. Kolodny. The power of priority: Noc based distributed cache coherency. In *Networks-on-Chip, 2007. NOCS 2007. First International Symposium on*, pages 117–126, May 2007.
- [2] Jörn Ostermann, Jan Bormans, Peter List, Detlev Marpe, Matthias Narroschke, Fernando Pereira, Thomas Stockhammer, and Thomas Wedi. Video coding with h. 264/avc: tools, performance, and complexity. *Circuits and Systems magazine, IEEE*, 4(1):7–28, 2004.
- [3] Kees Goossens, John Dielissen, and Andrei Rădulescu. The Æthereal network on chip: Concepts, architectures, and implementations. *IEEE Design & Test of Computers*, 22(5):414–421, Sep.-Oct. 2005.
- [4] Shaoteng Liu, A. Jantsch, and Zhonghai Lu. Analysis and evaluation of circuit switched noc and packet switched noc. In *Digital System Design (DSD), 2013 Euromicro Conference on*, pages 21–28, Sept 2013.
- [5] C. Paukovits and H. Kopetz. Concepts of switching in the time-triggered network-on-chip. In *Embedded and Real-Time Computing Systems and Applications, 2008. RTCSA '08. 14th IEEE International Conference on*, pages 120–129, 2008.
- [6] M.D. Harmanci, N.P. Escudero, Y. Leblebici, and P. Ienne. Providing qos to connection-less packet-switched noc by implementing diffserv functionalities. In *System-on-Chip, 2004. Proceedings. 2004 International Symposium on*, pages 37–40, Nov 2004.
- [7] Zheng Shi and Alan Burns. Real-time communication analysis for on-chip networks with wormhole switching. In *Proceedings of the Second ACM/IEEE International Symposium on Networks-on-Chip, NOCS '08*, pages 161–170, Washington, DC, USA, 2008. IEEE Computer Society.
- [8] Byungjae Kim, Jong Kim, SungJe Hong, and Sunggu Lee. A real-time communication method for wormhole switching networks. In *Parallel Processing, 1998. Proceedings. 1998 International Conference on*, pages 527–534, 1998.
- [9] S.L. Hary and F. Ozguner. Feasibility test for real-time communication using wormhole routing. *Computers and Digital Techniques, IEE Proceedings -*, 144(5):273–278, 1997.
- [10] Jong-Pyng Li and Matt W. Mutka. Real-time virtual channel flow control. *Journal of Parallel and Distributed Computing*, 32(1):49 – 65, 1996.
- [11] S. Balakrishnan and F. Ozguner. A priority-driven flow control mechanism for real-time traffic in multiprocessor networks. *Parallel and Distributed Systems, IEEE Transactions on*, 9(7):664–678, 1998.
- [12] Partha Kundu. On-die interconnects for next generation cmps. In *2006 Workshop on On- and Off-Chip Interconnection Networks for Multicore Systems*, Stanford, CA, USA, December 2006.
- [13] G. Michelogiannakis, D. Sanchez, W.J. Dally, and C. Kozyrakis. Evaluating bufferless flow control for on-chip networks. In *Networks-on-Chip (NOCS), 2010 Fourth ACM/IEEE International Symposium on*, pages 9–16, May 2010.
- [14] Hany Kashif, Hiren D. Patel, and Sebastian Fischmeister. Using link-level latency analysis for path selection for real-time communication on nocs. In *Proceedings of the Asia South Pacific Design Automation Conference (ASPDAC)*, pages 499–504, Sydney, Australia, February 2012.
- [15] Hany Kashif and Hiren Patel. Bounding buffer space requirements for real-time priority-aware networks. In *Proceedings of the Asia South Pacific Design Automation Conference (ASPDAC)*, SunTec, Singapore, January 2014.
- [16] Yue Qian, Zhonghai Lu, and Qiang Dou. Qos scheduling for nocs : Strict priority queueing versus weighted round robin. In *2010 IEEE INTERNATIONAL CONFERENCE ON COMPUTER DESIGN*, Proceedings IEEE International Conference on Computer Design, pages 52–59, 2010.
- [17] S. Chakraborty, S. Kunzli, and L. Thiele. A general framework for analysing system properties in platform-based embedded system designs. In *Design, Automation and Test in Europe Conference and Exhibition, 2003*, pages 190–195, 2003.
- [18] W. J. Dally and B. Towles. Route packets, not wires: On-chip interconnection networks. In *Proceedings of the 38th Design Automation Conference*, pages 684–689, Jun. 2001.
- [19] P. Poplavko, T. Basten, M. Bekooij, J. van Meerbergen, and B. Mesman. Task-level timing models for guaranteed performance in multiprocessor networks-on-chip. In *Proceedings of the 2003 international conference on Compilers, architecture and synthesis for embedded systems*, pages 63–72. ACM, 2003.
- [20] Y. Qian, Z. Lu, and W. Dou. Analysis of worst-case delay bounds for best-effort communication in wormhole networks on chip. In *Networks-on-Chip, 2009. NoCS 2009. 3rd ACM/IEEE International Symposium on*, pages 44–53. IEEE, 2009.
- [21] Gaoming Du, Cunqiang Zhang, Zhonghai Lu, Alberto Saggio, and Minglun Gao. Worst-case performance analysis of 2-d mesh nocs using multi-path minimal routing. In *Proceedings of the Eighth IEEE/ACM/IFIP International Conference on Hardware/Software Codesign and System Synthesis, CODES+ISSS '12*, pages 123–132, New York, NY, USA, 2012. ACM.
- [22] Sunggu Lee. Real-time wormhole channels. *J. Parallel Distrib. Comput.*, 63(3):299–311, March 2003.
- [23] D. Rahmati, S. Murali, L. Benini, F. Angiolini, G. De Micheli, and H. Sarbazi-Azad. Computing accurate performance bounds for best effort networks-on-chip. *Computers, IEEE Transactions on*, 62(3):452–467, 2013.
- [24] Ciprian Seiclescu, Dara Rahmati, Srinivasan Murali, Luca Benini, Giovanni De Micheli, and Hamid Sarbazi-Azad. Designing Best Effort Networks-on-Chip to Meet Hard Latency Constraints. *ACM Transactions on Embedded Computing Systems*, 12(4), 2013.
- [25] Evgeny Bolotin, Israel Cidon, Ran Ginosar, and Avinoam Kolodny. QNoC: QoS architecture and design process for network on chip. *Journal of Systems Architecture, Special Issue on Networks on Chip*, 50(2-3):105–128, Feb. 2004.
- [26] Zhonghai Lu, Axel Jantsch, and Ingo Sander. Feasibility analysis of messages for on-chip networks using wormhole routing. In *Proceedings of the Asia and South Pacific Design Automation Conference*, pages 960–964, Shanghai, China, Jan. 2005.
- [27] Zheng Shi. *Real-Time Communication Services for Networks on Chip*. PhD thesis, The University of York, 2009.
- [28] Jean-Yves Le Boudec and Patrick Thiran. *Network Calculus: A Theory of Deterministic Queuing Systems for the Internet*. Springer-Verlag, Berlin, Heidelberg, 2001.
- [29] M. Gries, C. Kulkarni, C. Sauer, and K. Keutzer. Comparing analytical modeling with simulation for network processors: a case study. In *Design, Automation and Test in Europe Conference and Exhibition, 2003*, pages 256–261 suppl., 2003.
- [30] D.B. Chokshi and P. Bhaduri. Modeling fixed priority non-preemptive scheduling with real-time calculus. In *Embedded and Real-Time Computing Systems and Applications, 2008. RTCSA '08. 14th IEEE International Conference on*, pages 387–392, 2008.
- [31] Andrei Hagiescu, Unmesh D. Bordoloi, Samarjit Chakraborty, Prahladavaradan Sampath, P. Vignesh V. Ganeshan, and S. Ramesh. Performance analysis of flexray-based ecu networks. In *Proceedings of the 44th Annual Design Automation Conference, DAC '07*, pages 284–289, New York, NY, USA, 2007. ACM.

- [32] Lothar Thiele, Ernesto Wandeler, and Samarjit Chakraborty. Performance analysis of multiprocessor dssps: a stream-oriented component model. *Signal Processing Magazine, IEEE*, 22(3):38–46, 2005.
- [33] Ernesto Wandeler and Lothar Thiele. Real-time calculus (rtc) toolbox. <http://www.mpa.ethz.ch/Rtctoolbox>, 2006.
- [34] N.E. Jerger and L.S. Peh. On-chip networks. *Synthesis Lectures on Computer Architecture*, 4(1):1–141, 2009.
- [35] W.J. Dally and S.G. Tell. The even/odd synchronizer: A fast, all-digital, periodic synchronizer. In *Asynchronous Circuits and Systems (ASYNC), 2010 IEEE Symposium on*, pages 75–84, May 2010.
- [36] E. Wandeler, L. Thiele, M. Verhoef, and P. Lieverse. System architecture evaluation using modular performance analysis: a case study. *INTERNATIONAL JOURNAL ON SOFTWARE TOOLS FOR TECHNOLOGY TRANSFER (STTT)*, 8(6):649–667, 2006.
- [37] Henrik Schiøler, Jan Jakob Jessen, Jens Dalsgaard Nielsen, and Kim Guldstrand Larsen. Network calculus for real time analysis of embedded systems with cyclic task dependencies. In *Proc. 20th International Conference on Computers and Their Applications, CATA 2005*, pages 326–332, 2005.
- [38] Lothar Thiele and Nikolay Stoimenov. Modular performance analysis of cyclic dataflow graphs. In *Proceedings of the Seventh ACM International Conference on Embedded Software, EMSOFT ’09*, pages 127–136, New York, NY, USA, 2009. ACM.
- [39] Anne Bouillard and Éric Thierry. An algorithmic toolbox for network calculus. *Discrete Event Dynamic Systems*, 18:3–49, March 2008.
- [40] Zheng Shi and A. Burns. Real-time communication analysis with a priority share policy in on-chip networks. In *Real-Time Systems, 2009. ECRTS ’09. 21st Euromicro Conference on*, pages 3–12, July 2009.
- [41] Jia Zhan, N. Stoimenov, Jin Ouyang, L. Thiele, V. Narayanan, and Yuan Xie. Designing energy-efficient noc for real-time embedded systems through slack optimization. In *Design Automation Conference (DAC), 2013 50th ACM / EDAC / IEEE*, pages 1–6, May 2013.
- [42] S. Manolache, P. Eles, and Zebo Peng. Buffer space optimisation with communication synthesis and traffic shaping for nos. In *Design, Automation and Test in Europe, 2006. DATE ’06. Proceedings*, volume 1, pages 1–6, March 2006.
- [43] Y. Ben-Itzhak, E. Zahavi, I. Cidon, and a. kolodny. Hnocs: Modular open-source simulator for heterogeneous nos. In *Embedded Computer Systems (SAMOS), 2012 International Conference on*, pages 51–57, July 2012.